



## UvA-DARE (Digital Academic Repository)

### The real role of active-shell in enhancing the luminescence of lanthanides doped nanomaterials

Wu, F.; Liu, X.; Kong, X.; Zhang, Y.; Tu, L.; Liu, K.; Song, S.; Zhang, H.

**DOI**

[10.1063/1.4809953](https://doi.org/10.1063/1.4809953)

**Publication date**

2013

**Document Version**

Final published version

**Published in**

Applied Physics Letters

[Link to publication](#)

**Citation for published version (APA):**

Wu, F., Liu, X., Kong, X., Zhang, Y., Tu, L., Liu, K., Song, S., & Zhang, H. (2013). The real role of active-shell in enhancing the luminescence of lanthanides doped nanomaterials. *Applied Physics Letters*, 102(24), Article 243104. <https://doi.org/10.1063/1.4809953>

**General rights**

It is not permitted to download or to forward/distribute the text or part of it without the consent of the author(s) and/or copyright holder(s), other than for strictly personal, individual use, unless the work is under an open content license (like Creative Commons).

**Disclaimer/Complaints regulations**

If you believe that digital publication of certain material infringes any of your rights or (privacy) interests, please let the Library know, stating your reasons. In case of a legitimate complaint, the Library will make the material inaccessible and/or remove it from the website. Please Ask the Library: <https://uba.uva.nl/en/contact>, or a letter to: Library of the University of Amsterdam, Secretariat, P.O. Box 19185, 1000 GD Amsterdam, The Netherlands. You will be contacted as soon as possible.

*UvA-DARE is a service provided by the library of the University of Amsterdam (<https://dare.uva.nl>)*

## The real role of active-shell in enhancing the luminescence of lanthanides doped nanomaterials

Fei Wu,<sup>1,2</sup> Xiaomin Liu,<sup>1,a)</sup> Xianggui Kong,<sup>1</sup> Youlin Zhang,<sup>1</sup> Langping Tu,<sup>1,2</sup> Kai Liu,<sup>1,2</sup> Shuguang Song,<sup>1</sup> and Hong Zhang<sup>3,a)</sup>

<sup>1</sup>State Key Laboratory of Luminescence and Applications, Changchun Institute of Optics, Fine Mechanics and Physics, Chinese Academy of Sciences, Changchun 130033, People's Republic of China

<sup>2</sup>Graduate University of the Chinese Academy of Sciences, Beijing 100049, People's Republic of China

<sup>3</sup>Van't Hoff Institute for Molecular Sciences, University of Amsterdam, Science Park 904, 1098 XH Amsterdam, The Netherlands

(Received 19 April 2013; accepted 21 May 2013; published online 18 June 2013)

Although it is widely recognized that doping sensitizers in the shell can improve significantly the luminescence of lanthanides doped nanocrystals, lack of an unambiguous picture of relevant luminescence enhancement mechanism seriously hinders the optimization of this approach. In this work, the complete processes of excitation energy migration, from photon absorption to emission, was dissected to unravel the role of sensitizers doped in shell in every individual stage. We revealed that the essence of doping sensitizers in the shell is just to increase the absorption efficiency whereas the quantum yield is lessened simultaneously. The optimal sensitizer doping concentration is also fixed to achieve the best luminescence performance.

© 2013 AIP Publishing LLC. [<http://dx.doi.org/10.1063/1.4809953>]

Lanthanides ( $\text{Ln}^{3+}$ ) doped nanocrystals (LnNCs) are emerging as an important class of nanomaterials owing to their wide applications in solid-state lasers,<sup>1,2</sup> three-dimensional flat panel displays,<sup>3–7</sup> and especially in biolabels<sup>8,9</sup> and bioimaging.<sup>10–13</sup> The unique capability of converting continuous-wave single-color near infrared (NIR) light into multi-color visible light makes these nanomaterials even more attractive in these applications. Compared with conventional biological labels, such as organic dye markers and quantum dots, LnNCs are superior in, e.g., high chemical stability, low toxicity, and high signal-to-noise ratio.<sup>14–16</sup> These advantages are, however, shrouded by the still low luminescence efficiency.<sup>17</sup> Yet efforts from all possible aspects, including nanohost and dopants, doping style, e.g., using multi-elements (sensitizer and emitter) codoping instead of single element doping. As far as the structure is concerned, core/shell structure has also been brought in aiming at improving the converting efficiency of the excitation light into luminescence. Growing a shell with similar lattice constants outside the core can protect the luminescent lanthanide ions in the core (especially those near the surface) from nonradiative losing energy to surface defects as well as vibrational deactivation from solvents or surface-bound ligands.<sup>18</sup> However, in majority of cases, the shell is inert, i.e., no dopant in the shell and its sole role is to minimize the probability of energy migration to the surface through lengthening the interaction distance. Most recently, it has been reported that active shell structure, i.e., containing sensitizers in the shell, could significantly enhance the luminescence.<sup>19–21</sup> These lanthanide doped core/active-shell nanoparticles (NPs) could enhance photoluminescence (PL) by several times higher than that of the core/inert-shell NPs of the same particle size. Despite the fact that the active shell

can provide the NPs with better luminescent performance in the context of highly required commercialization, the understanding of the role of active shell remains on its capacity to absorb more energy, leading to the great enhancement of luminescent intensity. The effect of the active shell on the dynamic equilibrium of the energy transfer, especially on the fluorescent quantum efficiency  $\eta_q$  was ignored, resulting in the blindness of the doping concentration of the sensitizer in the active shell, which used to be the same with that in the bare-core. Lacking of an unambiguous comprehension in relevant energy transfer dynamic process seriously hinders the optimization of the effective approach.

Herein, we have established a dynamic model for core/active-shell NPs to monitor the whole energy migration processes, from photon absorption to photon emission, and to analyze the role of sensitizers doped in shell in every individual stage. From the analysis of the relationship among the luminescence efficiency ( $\eta_{eff}$ ), absorption efficiency ( $\eta_a$ ), and fluorescent quantum efficiency ( $\eta_q$ ), we have revealed that, in this popular approach, the essence of active-shell strategy is just to increase the absorption efficiency whereas the quantum yield is reduced simultaneously. It can also be deduced from the model analysis that for the best luminescence performance, the optimal sensitizer doping concentration in the shell must be lower than that of the bare core. The  $\text{Ce}^{3+}$ ,  $\text{Tb}^{3+}$  co-doped  $\text{NaYF}_4$  core/active-shell NPs were first constructed and employed as a model system to validate the analysis and conclusions. Although downconversion process of  $\text{NaYF}_4:\text{Ce}^{3+}$ ,  $\text{Tb}^{3+}$  system was the target in this work for the sake of simplicity of study, the conclusions have also been proved in upconversion scenario. Our results shall shed insight on the proper employment of this very useful approach for improving optical properties of photonic nanomaterials.

A sensitizer and emitter co-doped model was established, as shown in Figure 1(a). Generally speaking, two processes are involved in the photoluminescence: the first is

<sup>a)</sup>Authors to whom correspondence should be addressed. Electronic addresses: x.liu@uva.nl and h.zhang@uva.nl.

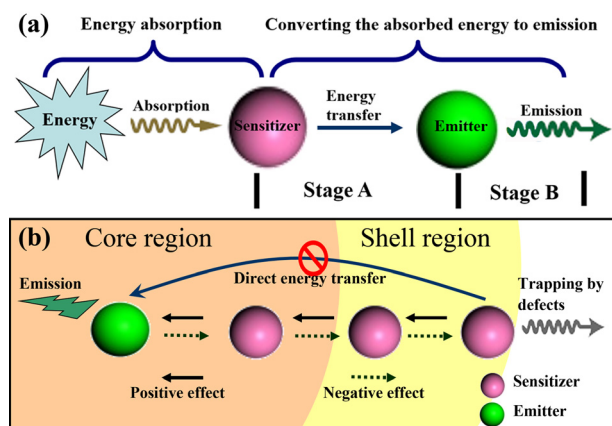


FIG. 1. (a) The luminescence processes in sensitizer and emitter co-doped nanoparticle. (b) The energy transfer kinetic processes from sensitizer to emitter in the case of core/active-shell structure.

the process of light absorption from pump source and the second is to convert the absorbed energy to emission. We suppose that  $\eta_a$  is the efficiency of the former process, i.e., the absorption efficiency.  $\eta_q$  is the efficiency of the latter process, namely, the luminescence quantum efficiency. Therefore,  $\eta_a = \text{number of absorbed photons}/\text{number of input photons}$ ;  $\eta_q = \text{number of emitted photons}/\text{number of absorbed photons}$ . Thus, the total luminescence efficiency  $\eta_{eff} = \eta_a \times \eta_q = \text{number of emitted photons}/\text{number of input photons}$ . In the core/active-shell NPs, the sensitizers doped in the shell can absorb additional excitation energy compared to the bare core and transfer it to the emitters in the core, resulting in the enhancement of  $\eta_a$ . To illustrate the effect of the sensitizers doped in shell on the  $\eta_q$ , the emission process can further be decomposed into two stages: stage A is the energy transfer process from the sensitizer to the emitter, and stage B is the emission process in the emitter. We assume that  $\eta_1$  is the quantum efficiency of stage A, defined as the number of the excited sensitizers involved in energy transfer divided by the total number of the excited sensitizers; and  $\eta_2$  is the quantum efficiency of stage B, i.e., the luminescence quantum efficiency of the emitter, thus the luminescence quantum efficiency  $\eta_q$  of such a nanoparticle can be described as  $\eta_q = \eta_1 \times \eta_2$ . In the core/active-shell NPs as illustrated in Figure 1(b), the sensitizers in the shell are close to the surface, increasing the possibility of trapping of excitation energy by surface related traps. Furthermore, these sensitizers are relatively far away from the emitters in the core; thus, the energy transfer from these sensitizers to the emitters is less efficient compared to the sensitizers in the core. The latter shall depress the luminescence quantum efficiency  $\eta_q$ . Thus, we can expect that, although the core/active-shell strategy may increase the energy absorbed efficiency  $\eta_a$ , the luminescence quantum efficiency is likely to be decreased in the mean time.

As mentioned above, the luminescent efficiency  $\eta_{eff}$  of the as-designed dynamic model depends on its excitation power absorbed efficiency  $\eta_a$  and luminescence quantum efficiency  $\eta_q$ . Increasing the sensitizer concentration shall lead more energy transferred to the emitters, which improves the absorbed efficiency  $\eta_a$ . This is the positive factor for the luminescence improvement. On the other hand, the distance

between the sensitizers will become shorter, which will make it easier for the absorbed energy to be transferred to surface traps, causing the dropping down of the luminescence quantum efficiency  $\eta_q$ , which is a negative factor for the luminescence improvement. Therefore, for the best luminescence performance, there shall be an optimal sensitizer concentration, which is a trade-off between these two contradictory effects. If we look into it in detail, the excited sensitizers in the shell of the core/active-shell NPs can not effectively transfer the energy to emitters, compared with the bare core NPs, due to the absence of the emitters in the shell, which will inevitably weaken the positive effect. On top of that, the energy migrates more among the excited sensitizers in shell and makes the trapping probability even higher, which will strengthen the negative effect. The decrease of the positive effect and the increase of the negative effect may result in the motion of the trade-off to the low concentration, namely depressing the optimal doping concentration. Therefore, we can estimate that the optimal concentration of sensitizers in shell must be lower than that of the sensitizers in the core.

To validate these concepts,  $\text{NaYF}_4: \text{Ce}^{3+}, \text{Tb}^{3+}$  NPs were chosen as a model system considering the important application of these materials in time-resolved Förster resonance energy transfer biosensor<sup>22,23</sup> and green light emitting devices.<sup>24,25</sup> Bare core, core/inert-shell and core/active-shell  $\text{NaYF}_4: \text{Ce}^{3+}, \text{Tb}^{3+}$  NPs were synthesized and their structure and morphology are well characterized (see supplemental material and Figure S1–S3).<sup>26</sup> The PL and UV-vis absorption spectra of the bare core, core/inert-shell, and core/active-shell NPs were recorded as shown in Figure 2. During the detection, the excitation power was kept the same for all samples. Thus, the luminescent efficiency  $\eta_{eff}$  and absorption efficiency  $\eta_a$  can be considered proportional to the emission and absorption intensities, respectively. The PL spectra and the corresponding photographs presented in Figure 2(a) clearly demonstrate the advantages of employing a core/active-shell structure over the bare core or the core/inert-shell nanoparticles. The most obvious difference lies in the intensity of the PL spectrum, in which the core/active-shell nanoparticles is approximately twice as high as that of the core/inert-shell and approximately 10 times higher than that of the bare core NPs. The spectra are normalized by the numbers of the nanoparticles. It can thus conclude that the core/active-shell NPs have the highest luminescence efficiency  $\eta_{eff}$ . Figure 2(b) shows the UV-vis absorption spectra of these three NPs ranging from 290 nm to 200 nm for sensitizer  $\text{Ce}^{3+}$ , among which the one of the active-shell NPs is the strongest due to the additional amount of sensitizers  $\text{Ce}^{3+}$  in the shell, which afford additional energy to  $\text{Tb}^{3+}$  in the core, verifying that the core/active-shell NPs has the highest absorption efficiency  $\eta_a$  (This was also proved by the excitation spectra as shown in Figure S4).<sup>26</sup>

We further compared the difference of luminescence quantum efficiency  $\eta_q$  of the bare core, core/inert-shell and core/active-shell NPs. The luminescence quantum efficiencies of the nanocrystals were determined by taking the  $\text{H}_2\text{SO}_4$  solution of quinine bisulfate (0.5 M) as reference (see supplemental material<sup>26</sup>) and keeping the absorptions of the samples the same at the excitation wavelength of 260 nm. By

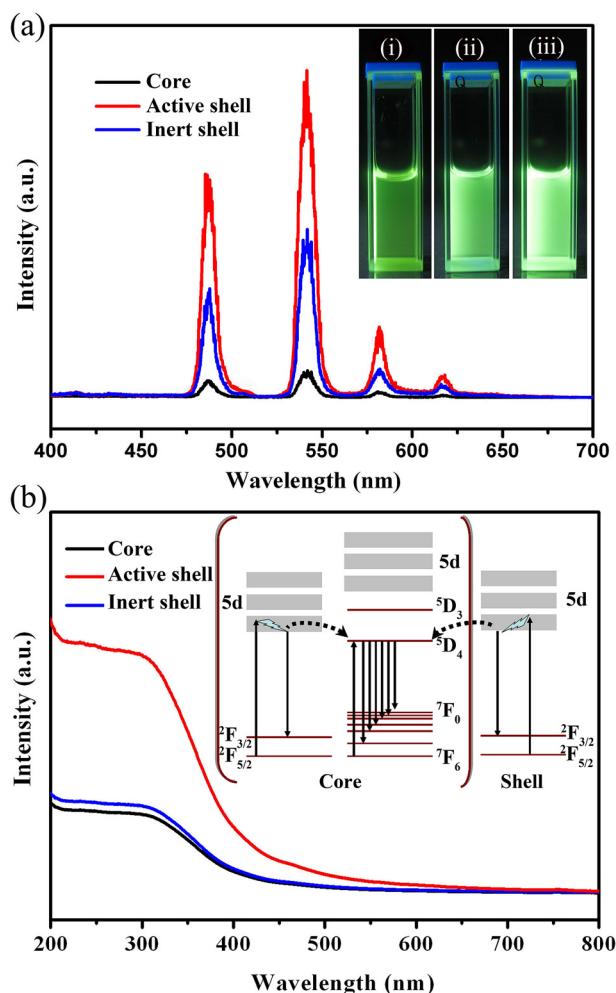


FIG. 2. (a) The PL spectra and the corresponding photographs of bare core NPs (I), inert-shell coated NPs (II) and active-shell coated NPs (III); (b) The UV-vis absorption spectra of these three NPs with the energy level diagrams of the core/active-shell NPs (insert). All the solutions are normalized by the numbers of nanoparticles.

measuring the luminescence of terbium, the fluorescent quantum efficiency of these NPs was determined to be 21.5% for bare core particles, 59.8% for core/inert-shell particles, and 53.2% for core/active-shell particles. These results tell us that the luminescence quantum efficiency  $\eta_q$  of core/active-shell NPs is indeed less than that of core/inert-shell NPs, in line with our hypothesis.

In the former model analysis, we have mentioned that the luminescence quantum efficiency  $\eta_q$  of such a core/active-shell NP can be described as  $\eta_q = \eta_I \times \eta_2$ . And we also have speculated that the phenomena of the relative lower luminescence quantum efficiency  $\eta_q$  in core/active-shell NPs was mainly caused by that the energy transfer from sensitizers in shell to the emitters is not efficient compared to the sensitizers in the core. In order to illustrate the difference between the energy transfer efficiency ( $\eta_I$ ) from  $\text{Ce}^{3+}$  to  $\text{Tb}^{3+}$  in the core region and in the active shell region, two model systems were designed (as shown in Figure 3). Model A was  $\text{NaYF}_4:40\% \text{Ce}^{3+}, 15\% \text{Tb}^{3+}/\text{NaYF}_4$ , where the  $\text{Ce}^{3+}$  ions were all distributed in the core. Model B was  $\text{NaYF}_4:15\% \text{Tb}^{3+}/\text{NaYF}_4:40\% \text{Ce}^{3+}$ , where the  $\text{Ce}^{3+}$  ions all located in the shell. The  $\text{Ce}^{3+}$  concentration in the core is the proven optimal concentration (40%) as evidenced in Figure S5(b).<sup>26</sup>

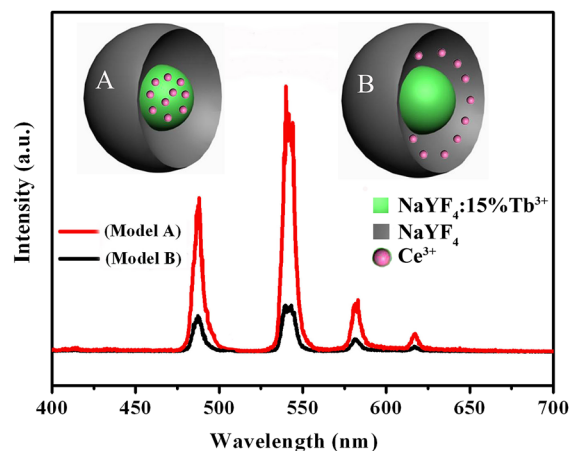


FIG. 3. PL spectra of model A and B. The spectra are normalized by the numbers of the nanoparticles.

The discrepancy of energy transfer efficiency ( $\eta_I$ ) of these two models can be featured in their photoluminescence under the same excitation power. It can be seen from Figure 3 that the PL of model A is much stronger than that of model B, indicating that the energy transfer efficiency ( $\eta_I$ ) in the shell region is less than that in the core region, which is responsible for the low quantum yield  $\eta_q$  in core/active-shell NPs compared to the core/inert-shell NPs.

To further document the emission efficiency of  $\text{Tb}^{3+}$  ( $\eta_2$ ) in these samples, we have tracked the temporal behavior of the green emission of  $\text{Tb}^{3+}$  (shown in Figure S6).<sup>26</sup> The lifetime of active-shell NPs was a little short compared with that of the inert-shell NPs, which may arise from the reverse energy transfer from  $\text{Tb}^{3+}$  to  $\text{Ce}^{3+}$  facilitated by the  $\text{Ce}^{3+}$  ions in the active shell, weakening the emission efficiency of  $\text{Tb}^{3+}$  ( $\eta_2$ ) and also resulting in the relative lower quantum yield  $\eta_q$  of active-shell NPs.

From the relationship among the luminescence efficiency  $\eta_{eff}$ , absorption efficiency  $\eta_a$ , and fluorescent quantum efficiency  $\eta_q$ , we have clearly proven that the reason of the enhancement of luminescence efficiency  $\eta_{eff}$  induced by active-shell strategy is actually just improving the pump source absorption efficiency  $\eta_a$ . The quantum yield  $\eta_q$  is not improved.

Now we turn to the dependence of the luminescence on the doping concentration of sensitizers in the active shell. Figure 4 exhibits the PL emission spectra of the  $\text{NaYF}_4:40\% \text{Ce}^{3+}, 15\% \text{Tb}^{3+}/\text{NaYF}_4: x\% \text{Ce}^{3+}$  colloidal solutions with the same concentration of  $\text{Tb}^{3+}$  ion under 260 nm excitation. Clearly, the luminescence of core/active-shell NPs boosts up with the increase of  $\text{Ce}^{3+}$  doping concentration and reaches a maximum value at 15% and then decreases. When it reaches 40% mole, i.e., the optimal doping concentration of sensitizers for bare core NPs (as evidenced in Figure S5<sup>26</sup>), the luminescence reduces markedly, even lower than that of core/inert-shell NPs, indicating that the negative effect is dominant. Therefore, for the best luminescence performance, doping concentration of the sensitizer  $\text{Ce}^{3+}$  in the active shell must be less than that in the core.

In the upconversion scenario, the energy transfer kinetic process from the sensitizer to emitter is much more complicated, however, still can be described as the schemes shown in Figure 1. The relationship among the  $\eta_{eff}$ ,  $\eta_a$ , and  $\eta_q$  is

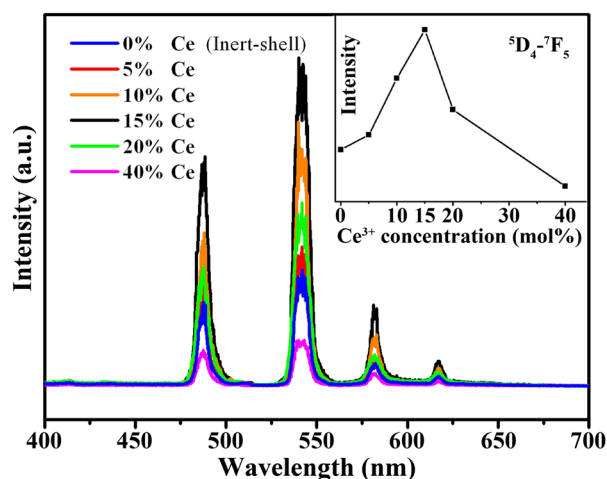


FIG. 4. PL spectra of the  $\text{NaYF}_4:\text{Ce}^{3+}$ ,  $\text{Tb}^{3+}/\text{NaYF}_4$ :  $x\%$   $\text{Ce}^{3+}$  colloidal solutions (0.1 M).

similar. Therefore, we have also extended and validated the conclusions to the upconversion scenario (see details in Figures S7 and S8).<sup>26</sup>

In conclusion, we have revealed that the essence of active-shell strategy, actually just increased the pump source absorption efficiency, the quantum yield was not improved. Furthermore, from the model analysis conclusion can be drawn that for the best luminescence performance, there exists an optimal concentration of sensitizers in the active shell which shall be less than that in the core. These concepts have been validated in down- and upconversion scenario separately. The findings described here strengthen the essential understanding of the luminescent enhancement induced by active-shell strategy, and afford a thread to improve the luminescent efficiency of photonic doping systems.

This work was financially supported by NSF of China (11004189, 11174277, 10904142, 61275202, and 61275197).

<sup>1</sup>F. Auzel, *Chem. Rev.* **104**, 139 (2004).

<sup>2</sup>C. K. Duan, P. A. Tanner, V. Babin, and A. Meijerink, *J. Phys. Chem. C* **113**, 12580 (2009).

- <sup>3</sup>E. Downing, L. Hesselink, J. Ralston, and R. A. Macfarlane, *Science* **273**, 1185 (1996).
- <sup>4</sup>F. Zhang, Y. Wan, T. Ying, F. Q. Zhang, Y. F. Shi, S. H. Xie, Y. G. Li, L. Xu, B. Tu, and D. Y. Zhao, *Angew. Chem., Int. Ed.* **46**, 7976 (2007).
- <sup>5</sup>F. Wang, Y. Han, C. S. Lim, Y. Lu, J. Wang, J. Xu, H. Chen, C. Zhang, M. H. Hong, and X. G. Liu, *Nature* **463**, 1061 (2010).
- <sup>6</sup>Y. P. Li, J. H. Zhang, X. Zhang, Y. S. Luo, S. Z. Lu, Z. D. Hao, and X. J. Wang, *J. Phys. Chem. C* **113**, 17705 (2009).
- <sup>7</sup>J. Limpert, F. Stutzki, F. Jansen, H. J. Otto, T. Eidam, C. Jauregui, and A. Tünnermann, *Light: Science & Applications* **1**, e8 (2012).
- <sup>8</sup>F. Van De Rijke, H. Zijlmans, S. Li, T. Vail, A. K. Raap, R. S. Niedbala, and H. J. Tanke, *Nat. Biotechnol.* **19**, 273 (2001).
- <sup>9</sup>F. Zhang, Q. H. Shi, Y. C. Zhang, Y. F. Shi, K. L. Ding, D. Y. Zhao, and G. D. Stucky, *Adv. Mater.* **23**, 3775 (2011).
- <sup>10</sup>F. Zhang, G. B. Braun, D. Y. Zhao, and G. D. Stucky, *Nano Lett.* **12**, 61 (2012).
- <sup>11</sup>Q. Ju, D. T. Tu, Y. S. Liu, R. F. Li, H. M. Zhu, J. C. Chen, C. Chen, M. D. Huang, and X. Y. Chen, *J. Am. Chem. Soc.* **134**, 1323 (2012).
- <sup>12</sup>J. C. Zhou, Z. L. Yang, W. Dong, R. J. Tang, L. D. Sun, and C. H. Yan, *Biomaterials* **32**, 9059 (2011).
- <sup>13</sup>C. Wang, L. Cheng, and Z. Liu, *Biomaterials* **32**, 1110 (2011).
- <sup>14</sup>F. Wang and X. G. Liu, *Chem. Soc. Rev.* **38**, 976 (2009).
- <sup>15</sup>D. Chatterjee, M. K. Gnanasamandhan, and Y. Zhang, *Small* **6**, 2781 (2010).
- <sup>16</sup>K. Liu, X. M. Liu, Q. H. Zeng, Y. L. Zhang, L. P. Tu, X. G. Kong, S. A. G. Lambrechts, M. C. G. Aalders, and H. Zhang, *ACS Nano* **6**, 4054 (2012).
- <sup>17</sup>J. C. Boyer and F. C. J. M. Veggel, *Nanoscale* **2**, 1417 (2010).
- <sup>18</sup>F. Wang, J. Wang, and X. G. Liu, *Angew. Chem., Int. Ed.* **49**, 7456 (2010).
- <sup>19</sup>X. M. Liu, X. G. Kong, Y. L. Zhang, L. P. Tu, Q. H. Zeng, and H. Zhang, *Chem. Commun.* **47**, 11957 (2011).
- <sup>20</sup>F. Vetrone, R. Naccache, V. Mahalingam, C. G. Morgan, and J. A. Capobianco, *Adv. Funct. Mater.* **19**, 2924 (2009).
- <sup>21</sup>D. M. Yang, C. X. Li, G. G. Li, M. M. Shang, X. J. Kang, and J. Lin, *J. Mater. Chem.* **21**, 5923 (2011).
- <sup>22</sup>H. Rajapakse, D. Reddy, S. Mohandessi, N. Butlin, and L. Miller, *Angew. Chem., Int. Ed.* **48**, 4990 (2009).
- <sup>23</sup>D. Geißler, L. J. Charbonnière, R. F. Ziessel, N. G. Butlin, H. G. L. Löhmansröben, and N. Hildebrandt, *Angew. Chem., Int. Ed.* **49**, 1396 (2010).
- <sup>24</sup>C. R. Ronda, T. Jüstel, and H. Nikol, *J. Alloys Compd.* **275–277**, 669 (1998).
- <sup>25</sup>C. Feldmann, T. Jüstel, C. T. Ronda, and P. J. Schmidt, *Adv. Funct. Mater.* **13**, 511 (2003).
- <sup>26</sup>See supplementary material at <http://dx.doi.org/10.1063/1.4809953> for experimental details, and XRD patterns, TEM images, EDX spectroscopy, excitation, and emission spectra of the prepared nanoparticles.